Evaluation of Radiation Damaged P-in-n and N-in-n Silicon Microstrip Detectors

Y. Unno[1], T. Yamashita[5], S. Terada[1], T. Kohriki[1], G. Moorhead[2], Y. Iwata[3], R. Takashima[4], M. Ikeda[3], E. Kitayama[5], K. Sato[3], T. Kondo[1], T. Ohsugi[3], I. Nakano[5], C. Fukunaga[6], P.W. Phillips[7], D. Robinson[8], L.G. Johansen[9], P. Riedler[10], S. Roe[10], S. Stapnes[11], and B. Stugu[9]

[1]Institute of Particle and Nuclear Studies, High Energy Accelerator Research Organiation (KEK), Tsukuba 305-0801, Japan
[2]School of Physics, University of Melbourne, Parkville, Victoria 3052, Australia
[3]Physics department, Hiroshima University, Higashi-Hiroshima 739-8526, Japan
[4]Education department, Kyoto University of Education, Kyoto 612-0863, Japan
[5]Physics department, Okayama University, Okayama 700-8530, Japan
[6]Physics department, Tokyo Metropolitan University, Hachiohji 192-0397, Japan
[7]Particle Physics department, Rutherford Appleton Laboratory, Chilton, Didcot, Oxon OX11 0QX, UK
[8]Cavendish laboratory, University of Cambridge, Cambridge CB3 0HE, UK
[9]Department of Physics, University of Bergen, N-5007 Bergen, Norway
[10]PPE, CERN, CH-1211 Geneve 23, Switzerland
[11]Department of Physics, University of Oslo, N-0316 Oslo 3, Norway

Abstract

Two p-in-n and one n-in-n silicon microstrip detectors were radiation-damaged and tested in a beam. A comparison was made between the p-in-n and the n-in-n in high resistivity wafers, and the p-in-n in a low and a high resistivity wafer. The charge collection showed a clear difference in the n-in-n and the p-in-n detectors, which suggested that the charge signals were shared between strips in the p-in-n detectors. Although a difference of the low and the high resistivity wafers was observed in the body capacitance measurement, little difference was observed in the beamtest results.

I. INTRODUCTION

In high energy hadron colliders, such as LHC, the number of particles generated at the interaction point is so large that the detectors installed near the interaction point need to be radiation-tolerant. The silicon microstrip detectors in the ATLAS detector will experience a fluence of 3×10^{14} particles/cm^2 over the 10 years of operation [1]. A radiation-tolerant design has been developed including the development of structures sustaining higher bias voltages and improvement in reducing the high electric field at the edges of implantation [2]. The radiation-tolerant silicon strip detectors developed have been evaluated, starting from the double-sided detector [3], and then the single-sided detectors with n-strip readout [4].

One of the major sources of radiation damage to the silicon detectors is the mutation of the bulk type from the initial n-type to p-type due to the creation of effective acceptor states in the bulk. Single-sided detectors with n-strip readout are efficient below full-depletion because the p-n junction is in the n-strip side after type-inversion. The detector, however, requires double-sided prrocessing in fabrication to make the initial p-n junction in the backside.

The p-readout was not considered first for two reasons: (1) it may require full-depletion to be efficient, and (2) it may not sustain high bias voltages. The second point needs an explanation. The p-readout single-sided silicon strip detector sustains the bias voltage in the p-n junction at the edge of p-strips and the p-bias ring surrounding the p-strips in the initial state. The backside is a planar densely doped n-layer (n^+). When the detector is sawed out, the interface of the planar n^+ and the silicon bulk is on the surface of the cutting edge. When the bulk type is inverted, the interface becomes the p-n junction. In the unirradiated detectors, the p-n junction on the surface of the cutting edge is known to break even with a small bias voltage.

Recent experience in the study of radiation tolerant silicon strip detectors has shown that the interface of the planar n^+ and the inverted p-bulk did not break at a low bias voltage, not even as high as several hundred volts. With the development of sustaining high bias voltages and the accumulation of knowledge of the charge collection in the p-strips in the radiation-damaged detectors, e.g., the p-side of the double-sided detector, it was becoming likely that the improved p-readout single-sided detector would work sufficiently for the application in the ATLAS experiment. The p-readout in the n-bulk silicon detectors had cost-advantage because of the simple backside processing.

Another interesting issue in the bulk damage was the increase of the depletion voltage in different resistivity wafers. The common resistivity of wafers of the silicon microstrip detectors had been 4 to 8 kΩcm, so-called “high resistivity” wafers. The low resistivity wafers, e.g., 1 kΩcm, had more donors. The radiation damage would create effective acceptors, and, if the donors were to remain, the donors would help to reduce the depletion voltage after type inversion. Although there was a report that the donors were removed at low fluences [5], it was important to confirm the result.

In this report, three silicon microstrip detectors were tested: one with p-readout in a high resistivity n-bulk wafer (p-in-n high), one with p-readout in a low resistivity n-bulk wafer (p-in-n low), and one with n-readout in a high resistivity n-bulk wafer (n-in-n high). These detectors were irradiated with protons and then subsequently put in a beamtest to evaluate the charge collection in the detectors.

II. DETECTOR SAMPLES

The p-in-n and n-in-n silicon microstrip detectors were fab-

ricated according to the ATLAS silicon microstrip detector specification [1]. One p-in-n detector (Sintef p-in-n: SinP10) [6] and one n-in-n detector (Ham n-in-n: HamN) [7] were made on high resistivity n-bulk wafers, 5 kΩcm and 4 kΩcm, respectively. One p-in-n detector was made on a low resistivity wafer, 1 kΩcm (Ham p-in-n: HamP) [7].

The detectors had a strip pitch of 80 μm and an outer dimension of 63.6 mm (width) x 64.0 mm (strip direction). The detector's parameters are summarized in Table 1. The nominal thickness of the detectors was 300 μm. The measured thicknesses were 293 μm, 300 μm, and 300 μm, for the Sintef p-in-n, the Ham p-in-n, and the Ham n-in-n detector, respectively, with a measurement error of about 1 μm.

Table 1.
Parameters of the p-in-n and n-in-n silicon strip detectors

Detector type:	AC-coupled, Single-sided
Bulk:	N-bulk, nominal 300 μm thickness
Resistivity:	High (4 or 5 kΩcm) and Low (1kΩcm)
Size (Outer):	6.36 cm × 6.4cm (width × length)
Strip area:	Width: 770 strips × 80μm =61.6 mm
Backside:	Uniformly doped n^+ layer
Strip parameters:	
Length:	62 mm
Strip pitch:	80 μm
Implant width:	16 μm
Resistance of implant:	≤100kΩ/cm
Readout pitch:	80 μm
AC coupling:	SiO2 + SiN
Width of Al. readout:	16 μm
Resistance of Al. readout:	≤20 Ω/cm
Bias resistance:	1.5±0.5 MΩ

III. PROTON IRRADIATION

A. Irradiation at KEK

The detectors were irradiated with 12 GeV protons in the EP1A beamline of the 12 GeV Proton Synchrotron at KEK [8]. The irradiation used the setup being developed for irradiations in the past [9]. The thermo-box stored the detectors and kept the temperature inside at -5 °C on average.

The nominal beam size was 61 mm full-width-half-maximum (FWHM) in the horizontal and 26 mm FWHM in the vertical. In order to cover the 6 cm x 6 cm detector area uniformly, the thermo-box was moved. The total intensity was counted with a secondary emission chamber (SEC) and triggered the stage movement. The absolute fluence was estimated from the activation of 1 cm x 1 cm Aluminium foils in a 5 x 5 matrix attached at the detector position.

In the run, there was a change of beam size which invalidated our calculation of the uniformity. With a correction to the movement, we could only achieve a fluence uniformity of ±16% at the maximum and minimum relative to the average in the readout region. The fluence variation with positions is shown in Figure 1. At the centre of the detector, the fluence was 4.2 x 10^{14} protons/cm^2, with an error of 10% which was dominated by the error in the cross section. In the subsequent beamtest, the readout region was set in the middle of the detector with an area of 2 cm x 2 cm horizontally and vertically. The detectors were kept cold, at -5 °C on average in the beamline, and stored at 0 °C after extraction.

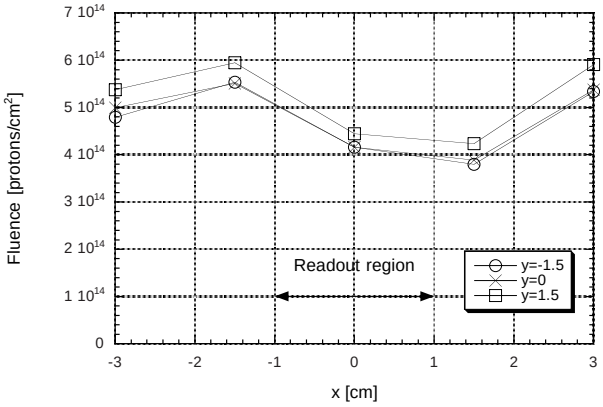

Figure 1: Proton fluence in the detector. The horizontal axis, x, is the position perpendicular to the strips and the parameter, y, is the position along the strip, in units of cm.

Before the beamtest, the irradiated detectors were warmed up for 5 days at room temperature because of the beamtest preparation and for 7 days at 28 °C in order to anneal the damage and to simulate the effects of the warm-up for maintenance in the real experiment. We have calculated that the full-depletion voltage will have increased by about 20% above the minimum full-depletion voltage.

The annealing and the anti-annealing of the full-depletion voltage was experimentally parameterized by H. Ziock [10]. Because of the different time dependence of the annealing and the anti-annealing effects, the full-depletion voltage first decreases and then increases. The change of the full-depletion voltage in time can be expressed by scaling the time with the characteristic time to reach the minimum, the time of minima. The temperature dependence of this time is shown in the bottom figure of Figure 2 and the full-depletion voltage at a fluence of 1x10^{14} p/cm^2 is shown in the top figure of Figure 2. The full-depletion voltage is parameterized to be linear with the fluence.

B. Capacitance measurement

After the warm-up, the body capacitance, i.e., the capacitance between the top and the bottom surface, was measured as a function of bias voltage. This is a common method to estimate the full-depletion voltage, using the corner between the theoretical $V^{-0.5}$ decrease and the saturation value, where V is the bias voltage. The environment temperature in the measurement was set at -15 °C in order to limit the leakage current. The measured

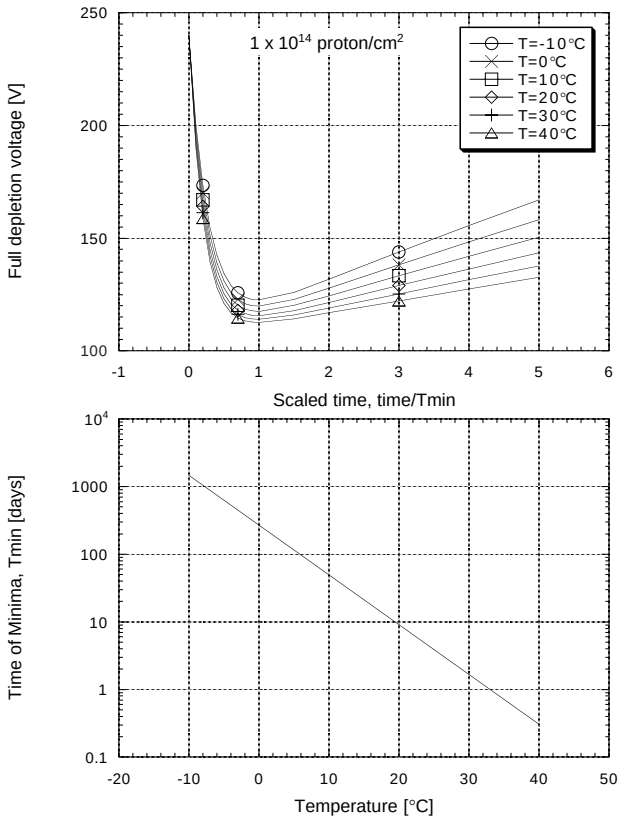

Figure 2: Expected full-depletion voltage as parameterized by H. Ziock as a function of time scaled by the characteristic time to the minimum (top figure), and the temperature dependence of this time (bottom figure)

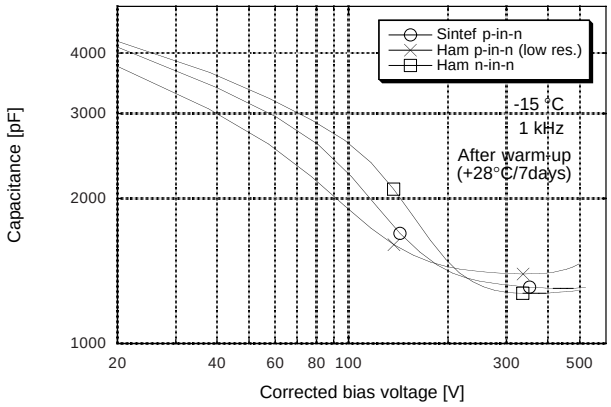

Figure 3: Body capacitances of the irradiated detectors as a function of the bias voltage after the warm-up. Sintef p-in-n (circle), and Hamamatsu n-in-n (square) were in the high resistivity bulk, and Hamamatsu p-in-n (cross) was in the low resistivity bulk wafer.

capacitances are shown in Figure 3.

The first impression was that the detector in the low resistivity wafer, HamP, had the lowest corner voltage, the p-in-n detector in the high resistivity wafer, SinP, the second, and the n-in-n in the high resistivity, HamN, the highest. This may suggest that the low resistivity wafer would develop lower full-depletion voltage than the high resistivity ones, and the p-n junction in strip geometry (radiation-damaged n-in-n detector) would require a higher voltages to deplete the bulk than the p-n junction in a planar one (radiation-damaged p-in-n).

However, as evident from the data, (1) the decrease of the capacitance was not monotonic and did not follow the theoretical expectation of $V^{-0.5}$, (2) the corner of the decreasing part and the saturation was very mild, and (3) the order of the saturated capacitances was opposite to the order of the capacitances in the decrease. Because of these observations, it was difficult to extract the corner voltage and, in turn, the full-depletion voltage.

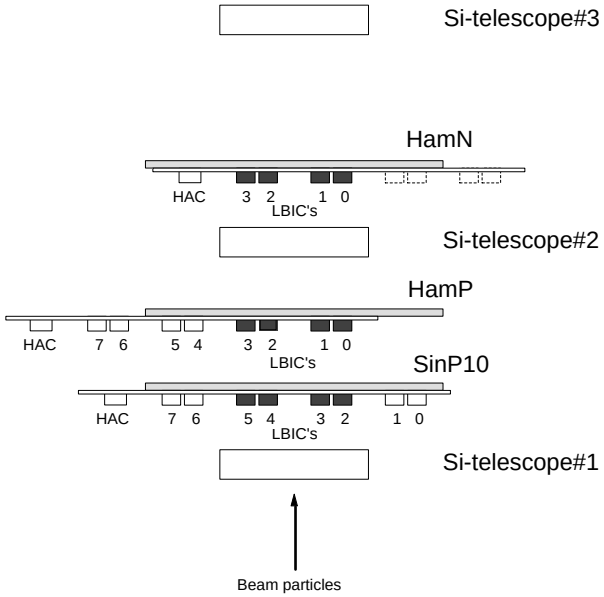

Figure 4: Beamtest setup of the irradiated detectors with the silicon strip detector telescopes which define the beam particle positions. The distance between each detector was about 30 mm.

IV. BEAMTEST

A. Setup

The irradiated detectors were tested in a beam at the π2 beamline of the 12 GeV proton synchrotron at KEK [11]. Negatively charged pi-mesons of 3 GeV/c were selected. The detectors were positioned in a thermo-box in the beamline as shown in Figure 4, together with the "Si-telescopes".

Each detector was connected to a readout hybrid which carried a fast-shaping electronics with on-off readout (binary readout) with the 64 channel bipolar amp-shaper-discriminator LSI chips (LBIC) and the 128 channel CMOS digital buffer LSI chips (CDP) [12]. The readout was interfaced via a communica-

tion chip, HAC, on the hybrid to the backend electronics and the data acquisition system. Because of limited available chips, only 4 LBIC's areas were readout in the middle of the detectors.

The irradiated detectors were sandwiched with silicon strip detectors instrumented with a Viking chips [13], "Si-telescopes", which provided a position resolution of 5 μm on the incident particles. The detectors were separated by about 30 mm. The smearing by multiple scattering [14] was less than 10 μm when the incident particle positions at the detectors were interpolated with the Si-telescopes.

B. Leakage currents

The environment of the thermo-box was kept at -17 °C in order to keep the leakage current small and prevent thermal runaway in the detector at higher bias voltages. The leakage current was monitored during the beamtest. A typical bias voltage dependence is shown in Figure 5.

All three detectors drew the same level of leakage current up to 500 V. The saturation bias voltage of the leakage currents seemed to be about 300 V for all three detectors.

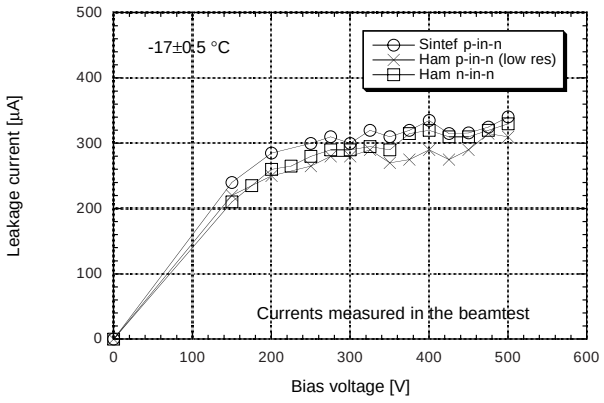

Figure 5: Leakage currents of the irradiated detectors during the beamtest. Environment temperature was set at -17 °C.

C. Charge collection

With one threshold in the electronics, only the efficiency of detecting signals above the threshold in a single strip can be obtained at a time. By scanning the thresholds, the pulse height (Landau) distribution was obtained in its integral form, convoluted with a Gaussian with a width characteristic of the system. An example of the threshold scan is shown in Figure 6.

The median of the Landau distribution was the threshold of 50% efficiency. In order to get the threshold, a modified error function, eq. (1), was fitted to the efficiency data.

$$eff(q) = p_3 \cdot \left(1 - erf\left(\frac{q - p_1}{p_2} f(q)\right)\right) \quad (1)$$

where

$$f(q) = max\left(0.6, 1 - p_4\left(\frac{q - p_1}{p_2}\right)\right). \quad (2)$$

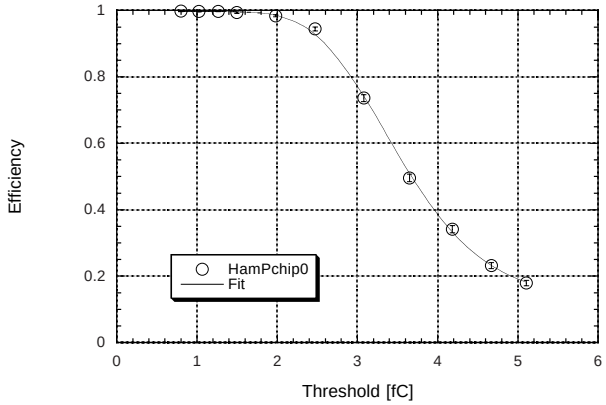

Figure 6: An example of a threshold scan for a channel in the Hamamatsu p-in-n detector. The efficiency curve was fit to a function described in the text and the median charge was defined as the threshold of 50% efficiency.

The function, *erf*, was the integral of the Gaussian distribution. The function, *f(q)*, is a phenomenological correction function to modify the Gaussian to the Landau distribution. The fitting parameters expressed the median (*p1*), the width (*p2*), the saturation (*p3*), and the skew (*p4*).

The median charges are shown as a function of bias voltages in Figure 7. A number of corrections were involved to reach this figure: (1) The median charges of each LBIC chips were scaled so that the average of the medians in the "strip region" at the bias voltages of 450, 475, and 500 V to be 3.5 fC. This was to correct the non-uniform radiation damage within a detector, and also correct the imperfect calibration of the amplifier responses. The definition of the "strip region" will be given in section D; (2) The bias voltages were corrected for the leakage current to give the bias voltages applied to the silicon bulk. There was a resistance of 11 kΩ in the bias power supply line externally; and (3) The bias voltages of the Sintef p-in-n detector were increased to correct the thickness by a simple theoretical expectation of $(300\ \mu m/293\ \mu m)^2$ which was to increase the bias voltages by 4.8%.

The data showed: (1) the p-in-n detectors required higher voltages to reach the same median charges as the n-in-n detector, and (2) two p-in-n detectors collected charges very similarly.

The first observation was the reflection of the location of the p-n junction after the type inversion: the p-n junction of the p-in-n detector was in the backside, while that of the n-in-n detector was in the strip side. Charge signals are induced in the strips when the real charges move along the electric field. In the p-in-n detector, the high electric field is near the backside which is several times the strip pitch away from the strips. The charge signals might thus have been shared between several strips. In the n-in-n detector, the highest electric field is near the strips and the charge signals are induced only one nearby strip. Circumstantial evidence was also obtained in the ratios of the median charges in the inter-strip over the strip regions in section D.

Since the n-in-n detector, after the type inversion, has the p-n junction in the readout side, the charge collection can be compared with the ideal diode, where the collected charges scales as the depletion depth, $V^{-0.5}$, and saturates once fully depleted. This ideal charge collection is plotted on Figure 7 with the full depletion voltage set at 300 V. The charge collection of the n-in-n detector was close to that of the ideal diode but slightly different, which could be caused by the strip structure of the electrodes and by the binary readout electronics.

The second observation is that there was very little difference in the charge collection between the low and the high resistivity wafers at the fluence in this test. Providing that the charge collection was reflecting the depletion depth and the fundamental property of the p-in-n detectors from two vendors was equal, there would be little difference in the full depletion voltages of the two wafers.

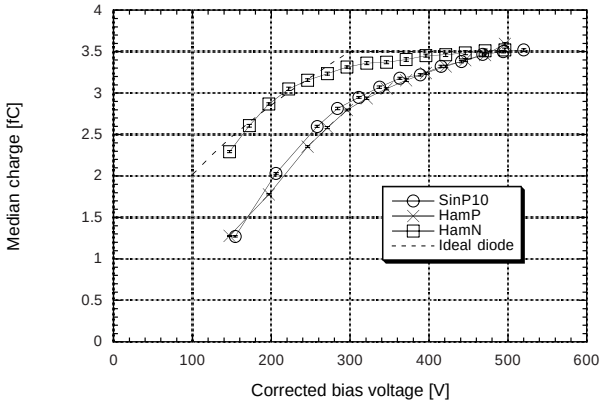

Figure 7: Median charges of the irradiated detectors as a function of bias voltages. The "ideal diode" is the theoretical expectation of the collected charges which scales as $V^{-0.5}$ and saturates at 300 V.

D. Charge collection in the inter-strip region

Electrons and holes liberated in the silicon bulk will travel along electric field lines. Charges ending-up midway between the strips induce charges in the two neighbour strips equally, i.e., the charges are shared between two strips.

The median charges were classified according to the beam particle positions. The positions midway between the strips, with a width of 20 μm, were defined as the inter-strip region. The positions around the strips, with a width of 40 μm, was defined as the strip region. The ratios of the median charges in the inter-strip over the strip regions are shown in Figure 8. Since the ratio was taken, the uncertainties associated with the non-uniform damage, imperfect calibration, etc. were largely eliminated.

The ratios of the n-in-n detector were insensitive to the bias voltage, while those of the p-in-n detectors were distinctively different: the ratio was much lower at low bias voltages and increased as the bias voltage increased to the level of the n-in-n detector near the highest voltages. This would be another indication that more charges were shared between strips in the p-in-n detectors.

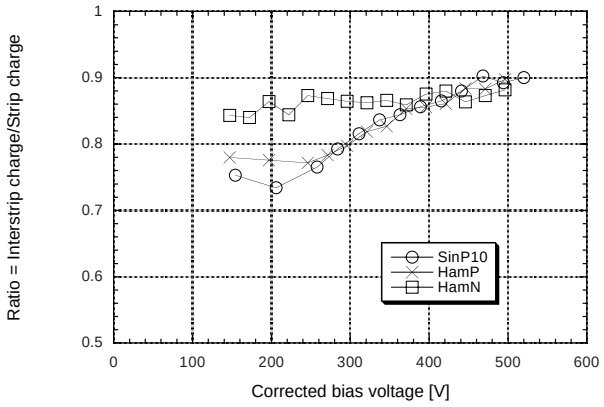

Figure 8: Ratios of the median charges in the inter-strip and the strip regions as a function of the bias voltage. The inter-strip region was defined as an area midway between the strips with a width of 20 μm, and the strip region as being around the strips with a width of 40 μm.

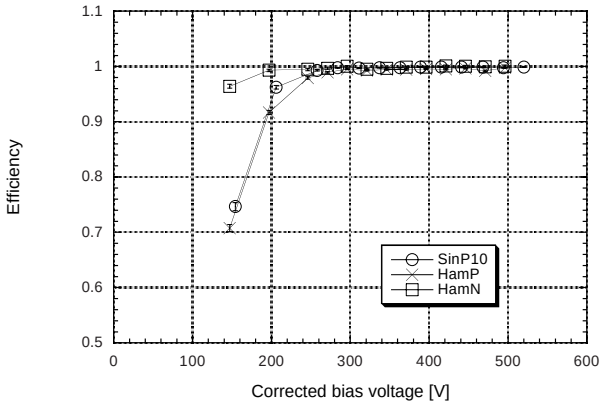

Figure 9: Bias voltage dependence of the efficiency at the threshold of 1 fC.

E. Efficiency at 1 fC

In a real experiment, the data taking will be made by setting the threshold at one point. From the efficiency and electronics noise argument, the threshold is to be set around 1 fC. The bias voltage dependence of the efficiency at a threshold of 1 fC is shown in Figure 9. The p-in-n detectors, although requiring larger bias voltages than the n-in-n detector, became efficient (>99%) above a bias voltage of 250 V.

V. SUMMARY

Two p-in-n and one n-in-n silicon microstrip detectors of the ATLAS silicon microstrip detector specification were irradiated and tested in a beam. Two comparisons motivated the study: a

comparison of p-in-n and n-in-n detectors, and a comparison of low and high resistivity wafers. The resistivities of the wafers were 1 kΩcm for the low resistivity and 4 or 5 kΩcm for the high resistivity wafers. The proton fluence was 4.2×10^{14} p/cm^2. The detectors were kept cold during the irradiation and stored cold.

The irradiated detectors were warmed up to anneal and to simulate the warm-up in the maintenance in the real experiment. The body capacitance measurement implied that the low resistivity wafer had a lower corner voltage. However, the voltage was not a clear evidence of a lower full-depletion voltage. In the beamtest, the detectors were read out with fast-shaping electronics with one-threshold. By scanning the threshold, charge collection information in a single strip was obtained. The median charges showed that the full-depletion voltage would be around 300 V in the n-in-n detector. The leakage currents suggested all three detectors had a similar full-depletion voltage at around 300 V.

There was no clear saturation in the median charges in the p-in-n detectors. The p-in-n detectors required larger bias voltages (by 70~100V) to reach the same median charges as the n-in-n detector. The ratios of the median charge in the interstrip over the strip regions showed larger charge loss in the p-in-n detectors at low bias voltages. These observations would suggest that the charges were shared between several strips in the p-in-n detectors.

The two p-in-n detectors on low and high resistivity wafers behaved very similarly. Although the full-depletion voltages of the two detectors were not evident in the charge collection, the similarity suggested that there was little difference in the full-depletion voltages of the different resistivity wafers, providing the fundamental character of the detectors from the two manufacturers was the same.

The p-in-n detectors required a higher bias voltage for full charge collection, however, the efficiency at 1 fC showed that the detectors were efficient once the bias voltage was over 300 V.

VI. Acknowledgement

The authors wish to acknowledge the cooperation of the beam channel crews of the EP1A and π2 beamline of the KEK PS for the irradiation and the beamtest. This work was supported by Japan Ministry of Education, Science, and Culture, Japan Society for Promotion of Science, Australian Research Council, and UK Particle Physics and Astronomy Research Council.

VII. References

[1] ATLAS Inner Detector Technical Design Report, CERN/LHCC/97-17, ATLAS TDR 5, 30 April 1997

[2] T. Ohsugi et al., “Micro-discharge noise and radiation damage of silicon microstrip sensors”, Nucl. Instr. Metho. A383, pp. 166-173, 1996

[3] Y. Unno et al., “Characterization of an Irradiated Double-sided Silicon Strip Detector with Fast Binary Readout Electronics in a Pion Beam”, IEEE Trans. Nucl. Scie., Vol. 43, pp. 1175-1179, 1996

[4] Y. Unno et al., “Beam Test of a Large Area N-on-n Silicon Strip Detector with Fast Binary Readout Electronics”, IEEE Trans. Nucl. Scie., Vol. 44, pp. 736-742, 1997; Y. Unno et al., “Evaluation of P-stop Structures in the N-side of N-on-n Silicon Strip Detector”, IEEE Trans. Nucl. Scie., Vol. 45, pp. 401-405, 1998

[5] D. Pitzl et al., “Type inversion in silicon detectors”, Nucl. Instr. Metho. A311, pp. 98-104, 1992

[6] SINTEF Electronics and Cybernetics, P. O. Box 124 Blindem, N-0314 Oslo, Norway

[7] Hamamatsu Photonics, 1126-1, Ichino-cho, Hamamatsu-shi 435, Japan

[8] S. Terada et al., “Proton irradiation on silicon detectors and related materials”, T363, KEK test experiment

[9] S. Terada et al., “Proton irradiation on p-bulk silicon strip detectors using 12 GeV PS at KEK”, Nucl. Instr. Metho. A383, pp. 159-165, 1996

[10] H.-J. Ziock et al., “Temperature dependence of the radiation induced change of depletion voltage in silicon PIN detectors”, Nucl. Instr. Metho. A342, pp. 96-104, 1994

[11] Y. Unno et al., “Beamtest of the radiation-damaged silicon microstrip detectors”, T429, KEK test experiment

[12] LBIC: E. Spencer et al., “A Fast Shaping Low Power Amplifier-Comparator Integrated Circuit for Silicon Strip Detectors”, IEEE Trans. Nucl. Scie., Vol. 42, pp. 796-802, 1995; CDP: J. DeWitt, “A Pipeline and Bus Interface Chip for Silicon Strip Detector Read-out”, Proc. IEEE Nucl. Scie. Symp., San Francisco, CA., Nov. 1993

[13] O. Toker, S. Masciocchi, E. Nygard, A. Rudge, P. Weilhammer, “Viking: A CMOS low noise monolithic 128-channel frontend for Si strip detector readout”, Nucl. Instr. Metho. A340, pp. 572-579, 1994

[14] Particle Data Group, “Review of Particle Physics”, Eur. Phys. J. C3, pp. 146, 1998